

Flow Through Openings in Width Constrictions

GEOLOGICAL SURVEY WATER-SUPPLY PAPER 1369-D



Flow Through Openings in Width Constrictions

By JACOB DAVIDIAN, P. H. CARRIGAN, JR., and JOHN SHEN

RIVER HYDRAULICS

GEOLOGICAL SURVEY WATER-SUPPLY PAPER 1369-D

A laboratory study to define the discharge characteristics, flow-distribution pattern, and backwater effects of open-channel constrictions with several openings



UNITED STATES DEPARTMENT OF THE INTERIOR

STEWART L. UDALL, *Secretary*

GEOLOGICAL SURVEY

Thomas B. Nolan, *Director*

CONTENTS

	Page
Abstract.....	91
Introduction.....	91
Objectives.....	92
Review of previous work.....	92
Scope.....	93
Laboratory equipment.....	93
Notation.....	95
Flow pattern.....	95
Discharge characteristics.....	97
Preliminary considerations.....	97
Separate-opening procedure.....	101
Division into single-opening units.....	101
Coefficient of discharge.....	102
Determination of h_1	102
Determination of h_3	104
Variation of discharge coefficient.....	104
Flow distribution.....	108
Backwater effects.....	112
Separate-opening procedure.....	113
Backwater-contraction factor.....	113
Backwater ratio, basic condition.....	114
Effect of constriction geometry.....	114
Evaluation of Δh_a	116
Multiple-opening procedure, basic-type constrictions.....	119
Symbols.....	120
Literature cited.....	122

ILLUSTRATIONS

	Page
PLATE 4. Variation of surface level, backwater, and backwater ratio with number of openings.....	In pocket
FIGURE 14. General view of the experimental flume.....	94
15. Typical constriction in the flume.....	94
16. Typical multiple-opening constriction in a rectangular chan- nel.....	96
17. Variation of discharge coefficient with opening-width ratio, two-opening constriction.....	100
18. Comparison of computed and observed stagnation levels.....	104
19. Comparison of coefficients for two-opening constrictions in a rectangular channel.....	105

	Page
FIGURE 20. Comparison of coefficients for 3-, 4-, and 5-opening constrictions in rectangular channels.....	106
21. Comparison of coefficients for 2- and 3-opening constrictions in nonrectangular channels.....	107
22. Variation in channel shape.....	107
23. Influence of effective-opening area on discharge distribution..	110
24. Effect of relative channel roughness on distribution of discharge.....	111
25. Backwater ratio for basic-type constrictions; 2, 3, 4, and 5 openings.....	115
26. Comparison of k_e for single- and multiple-opening constrictions.....	117
27. Backwater ratio for separate openings, nonbasic-type constrictions.....	118
28. Backwater ratio for multiple-opening system, basic-type constrictions.....	120

TABLE

	Page
TABLE 1. Range in geometric and hydraulic variables.....	108

RIVER HYDRAULICS

FLOW THROUGH OPENINGS IN WIDTH CONSTRICTIONS

BY JACOB DAVIDIAN, P. H. CARRIGAN, JR., and JOHN SHEN

ABSTRACT

A highway embankment across a stream channel may have one or several bridge openings. In 1953, the pattern of flow through a single opening was quantitatively described by C. E. Kindsvater, R. W. Carter, and H. J. Tracy. The present investigation of the flow pattern at constrictions with two to seven openings is a continuation of the earlier study. Laboratory experiments and the analysis were directed toward the development of methods for (a) computing discharge through multiple-opening constrictions, (b) apportioning a given total discharge among the several openings, and (c) predicting the backwater caused by the constriction.

The division of flow among the openings was related to the relative area of each opening, and the relative velocity in the channel immediately upstream from each opening. On the basis of this relationship, the boundaries of the flow channel approaching each opening were established. The head-discharge and backwater characteristics of each opening were then analyzed separately. It is shown that the relations developed for the constriction with a single opening are applicable to each opening of a multiple-opening constriction once the boundaries of the separate flow channels have been established.

INTRODUCTION

A better knowledge of the pattern of flow through constrictions formed by the crossings of highways and stream channels is becoming increasingly important to hydraulic engineers. This knowledge is used in the design of the location and size of bridge openings and in the computation of velocity of flow and backwater for a given discharge. Another important application is found in the determination of the peak discharge of floods from a survey of high-water marks and the geometry of the channel and constriction. This method of peak-flow determination is frequently used by the U.S. Geological Survey.

This study of flow through multiple-opening constrictions is a continuation of a laboratory investigation that began in 1951. The initial part of the investigation, which dealt with flow through single-

opening constrictions, has been reported by Kindsvater and others (1953), Kindsvater and Carter (1955), and Tracy and Carter (1955).

The work on which this report is based was part of the research program of the Surface Water Branch, Water Resources Division. The early part of the laboratory study and analysis was conducted by Jacob Davidian, hydraulic engineer. The work was completed by P. H. Carrigan, Jr., and John Shen. Others who have participated are F. H. Ruggles, Jr., F. A. Kilpatrick, and C. M. Lester. The study was conducted under the direct supervision of H. J. Tracy.

OBJECTIVES

The objectives of the study of multiple-opening constrictions are to develop methods for (a) the computation of discharge through multiple-opening constrictions, (b) the apportionment of a given total discharge among the several openings, (c) the prediction of the maximum backwater caused by the constriction.

REVIEW OF PREVIOUS WORK

The first comprehensive research on the flow of water through open-channel constrictions was conducted by Kindsvater and Carter (1955). In that work, a solution of a discharge equation for flow through single-opening constrictions was developed. The variation of a coefficient of discharge was shown to be dependent upon several dimensionless variables. The influences of these variables were determined experimentally. In that study only vertical-faced constrictions were investigated.

The description of the discharge characteristics of single-opening constrictions was extended by Kindsvater, Carter, and Tracy (1953) to include a greater range of boundary forms. Procedures for collecting field data and applying the data to the solution of the discharge equation were also suggested.

The backwater effects of single-opening constrictions in open channels were studied by Tracy and Carter (1955). The backwater was defined as the difference in elevation between the normal- and the constricted-surface profile at a nominal approach section. Results of that study were summarized in the form of a backwater ratio, which is the ratio of backwater to the water-surface drop through the constriction. This backwater ratio was determined experimentally to be a function of channel roughness, percentage of channel contraction, and constriction geometry.

Subsequently, Liu, Bradley, and Plate (1957) presented an alternate solution for backwater. The backwater was referenced as a ratio either (a) to the normal flow depth or (b) to the velocity head at the most contracted section. Laboratory tests were made to describe the

variation in backwater ratio with variations in channel slope, in channel roughness, in abutment shape and length, in degree of channel contraction, in Froude number, and in depth of flow. The effect of dual, parallel constrictions was also considered.

SCOPE

In the present investigation, tranquil, steady flows through open channel constrictions having two to seven openings were studied. The channels were rigid and prismatic. A variety of abutment and channel shapes were tested. The effect of channel roughness was investigated in considerable detail.

LABORATORY EQUIPMENT

Laboratory tests for this investigation were conducted in the hydraulics laboratory at the Georgia Institute of Technology.

The tests were made in a horizontal steel-walled flume 80 feet long, 14 feet wide, and 2 feet deep. A 3-foot section in the center of the channel is depressed 6 inches below bed level to simulate a main channel with overbank flow. The depressed central channel may be covered with metal plates to form a full-width rectangular channel. Other changes in the channel cross section were made by using built-up floor sections of Transite. The width of the channel was varied by using aluminum false walls sealed to the concrete floor. A general view of the flume is shown in figure 14, and a typical constriction, in figure 15.

Water from a constant-head tank discharges into the forebay of the flume upstream from a full-width thin-plate weir. It then passes through two rows of 1- by 3-inch vertical-strip baffles spaced on 6-inch centers, and next through two sets of expanded-metal screens. The forebay is 5.5 feet long. The end of the forebay is 31 feet upstream from the model section. The discharge into the flume was measured with a gravimetrically calibrated venturi meter located in the supply piping.

Water-surface levels were measured with point gages equipped with scales and verniers graduated to 0.001 foot or 0.01 centimeter. The elevations of the floor and the system of rails, carriages, and rollers supporting the point gages were established and checked at intervals with an engineer's level.

Velocities were measured with small current meters calibrated in a towing tank and with pitot tubes calibrated in the efflux from an orifice.

Constrictive elements were made of metal, wood, and Transite. The linear dimensions of the constrictions were determined to the nearest 0.002 foot.



FIGURE 14.—General view of the experimental flume.

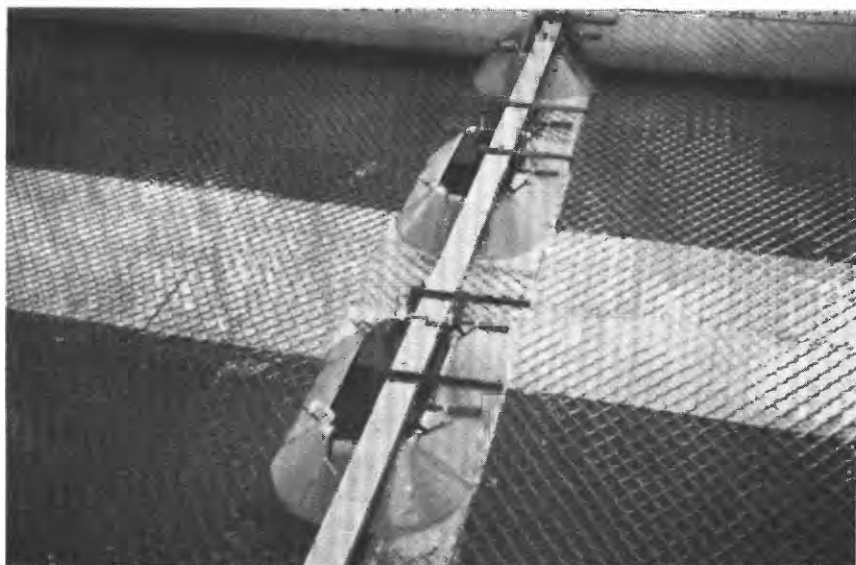


FIGURE 15.—Typical constriction in the flume.

The bed roughness was varied by using different combinations of diamond-mesh chain-link wire fencing and expanded-metal inserts fastened to the concrete floor. Five different degrees of bed roughness were used. For the cases of smooth concrete floor and one layer of 2-inch diamond-mesh wire fencing, the computed values of the Man-

ning coefficient n were 0.012 and 0.025 respectively. These values of n remained essentially constant over the range of depth used in the tests. For other types of roughness, however, the values of n varied with the depth. The value of n for two layers of wire fencing ranged from 0.031 at a depth of 0.75 foot to 0.046 at a depth of 0.35 foot. For a similar range in depth, the value of n for the expanded-metal inserts placed in every third diamond mesh ranged from 0.048 to 0.072; and for inserts in every second mesh, from 0.065 to 0.115.

NOTATION

The letter symbols used in this report are defined in the illustrations, in the text, and on pages 120–122. Many of the symbols adapted in the present report are the same as those defined in the report on flow through single-opening constrictions (Kindsvater and others, 1953).

FLOW PATTERN

A definition sketch for flow through a typical multiple-opening constriction in a rectangular channel is shown in figure 16. At some upstream section (section 0), the flow is undisturbed and the flow distribution is governed by the channel characteristics. Approaching the vicinity of the constriction, the flow decelerates as the depth increases. The deceleration process continues until a section (designated section a) is reached. Farther downstream the flow begins to accelerate unevenly owing to the effect of the constriction and eventually undergoes a redistribution process. At section 1, the approach section for each opening, the flow pattern is essentially dominated by the constriction geometry. As the fluid passes through each opening, the live stream contracts to a width somewhat less than that of the opening, and the corresponding average longitudinal profile drops sharply. At the section of minimum width of each live stream (section 2), the expansion process begins and continues until normal flow is again established at some distance downstream (section 4).

On the upstream side of the constriction embankments, partial stagnation occurs in the corners formed by the junction of the embankments and the side boundaries of the channel. Stagnation occurs at each of the interior embankments (those not joined to the side boundaries), in which case the flow stagnates along an approximately vertical line. The location of this line is a function of the arrangement and geometry of the constriction, and of the hydraulic characteristics of the approach channel. The flow divides at the stagnation lines and passes through the openings on each side.

As a related circumstance, shear along the channel boundaries, acting in conjunction with the deceleration of the flow, causes separation. In the corner regions, sizeable separation zones with eddies are

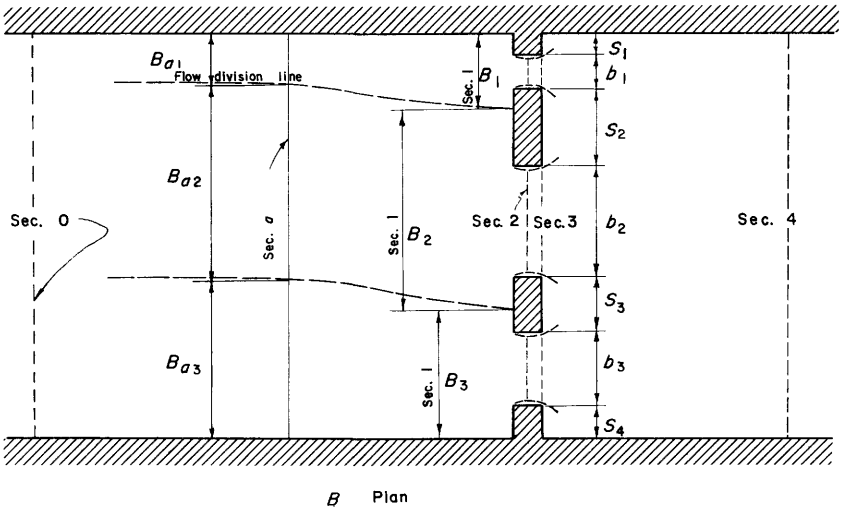
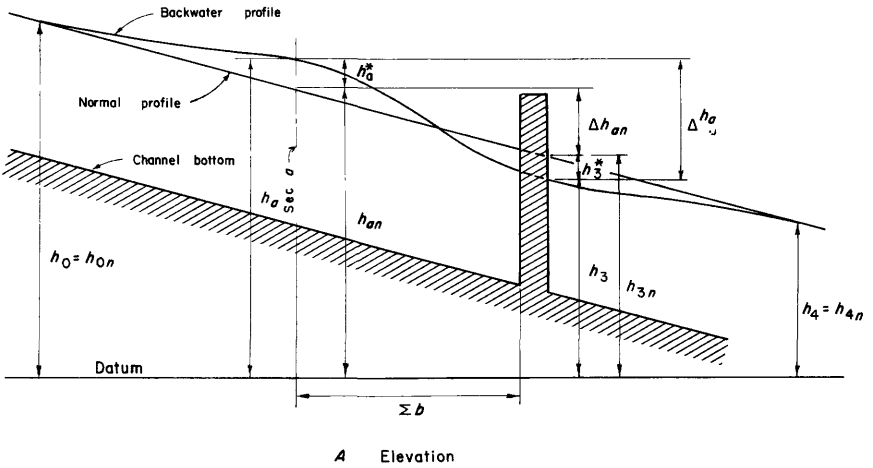


FIGURE 16.—Typical multiple-opening constriction in a rectangular channel.

created. The energy required to maintain the eddy motion in these zones prevents the occurrence of the full stagnation head in the corner. At the interior embankments, separation occurs along the floor near the stagnation lines. The extent of the separation is, however, much smaller at the interior embankment than in the corner. The energy losses are also apparently insignificant, as virtually the full stagnation level is measured at the embankment. On both sides of the stagnation lines, the piezometric head decreases in the direction of flow, and the fluid moves along the faces of the embankments to the ends without further separation.

In this connection, two sets of slow-moving rollers with horizontal axes are formed at each side of the stagnation line on each interior embankment. As the flow stagnates, a part of the fluid in the upper layers of the flow moves upward along the embankment face, turns upstream near the surface to oppose the mean motion, and then disappears below the surface a short distance upstream. A similar eddy motion, rotating in the opposite direction, is observed in the lower part of the flow. The eddy motion persists in the form of spiral rollers as the fluid moves toward the ends of the embankments. The rollers are ultimately swept through the constriction openings.

At the section of maximum contraction, the live stream from each of the openings begins to expand. For a short distance downstream, the average paths of the streams are well defined and, in contrast to the stream from the single-opening constriction, shift from side to side with a regular and repeated motion as vortexes are alternately formed and shed at the sides of the live streams. As a part of the interrelated system of events, the piezometric head at the downstream edge of each abutment fluctuates in an orderly fashion to correspond with the motion of the adjoining live stream. Boundary roughness plays an important role in the downstream pattern of motion. The vortex formation and the attendant oscillation of the efflux from the openings may be very pronounced for smooth channels. As the channel is progressively roughened, the motion becomes less intense and eventually becomes imperceptible.

DISCHARGE CHARACTERISTICS

PRELIMINARY CONSIDERATIONS

Problems in rapidly varied flow are usually not amenable to rigorous mathematical analysis. For such cases, methods of dimensional analysis may be used in conjunction with laboratory experiment to obtain practical solutions. The problem of flow through open-channel constrictions is of this nature.

It is generally recognized that in the region of rapid acceleration near a constriction, the influences of viscosity as well as surface tension can be assumed to be relatively insignificant. Thus, the following variables are considered to be sufficient in describing the discharge characteristics of flow through a multiple-opening constriction having vertical embankments and square-edged abutments, and located in a smooth, rectangular channel:

$$Q, \Delta h, g, L, \Sigma b, B, b_1, b_2, \dots, b_{n-1}, S_1, S_2, \dots, S_n, y_3.$$

In this array, Q is the total discharge; Δh is the difference in surface levels between an approach section and the section of maximum

contraction; g is the acceleration of gravity; L is the length of the abutment; Σb is the sum of the opening widths; B is the width of the channel; b is the width of an opening; S is the width of an embankment; n is the number of embankment sections; and y_3 is the average depth at section 3. Section 3 is located at the downstream side of the constriction. The piezometric level at section 3 is essentially equivalent to the level of the water surface at section 2, the section of maximum contraction of the live streams. The location of the points at which the surface level at section 3 is measured is discussed subsequently.

The variables listed above may be combined by methods of dimensional analysis to give a minimum number of significant ratios:

$$C = \frac{Q}{y_3 \Sigma b \sqrt{g \Delta h}} = f \left(\frac{Q}{y_3 \Sigma b \sqrt{g y_3}}, \frac{\Sigma b}{B}, \frac{L}{\Sigma b}, \frac{y_3}{\Sigma b}, \frac{S_1}{\Sigma b}, \dots, \frac{S_n}{\Sigma b}, \frac{b_1}{\Sigma b}, \dots, \frac{b_{n-1}}{\Sigma b} \right). \quad (1)$$

The dependent ratio and the first four independent ratios of equation 1 are, in order, a coefficient of discharge, a Froude number, a contraction ratio, the length-width ratio of the openings, and the depth-width ratio of the openings. The remaining ratios are descriptive of the distribution of the total opening width among the several openings of the constriction.

The term Σb is analogous to the opening width b of the single-opening constriction. The first four independent ratios of equation 1 are thus the multiple-opening equivalents of the ratios selected by Kindsvater and Carter to describe the discharge characteristics of single-opening constrictions. Of these four, only the ratio y_3/b was found to have an insignificant influence on the single-opening flow pattern. It is thus reasonable to assume that the counterparts of the remaining three ratios may not be excluded from consideration in the present case. Therefore, unless the ratios descriptive of the opening-width distribution can be shown to be unimportant in their effect on the discharge coefficient, and hence effectively eliminated, the experimental solution of equation 1 would be impractical because of the great number of these ratios involved. Some observations regarding the effect of these variables, based upon exploratory tests, are contained in the following paragraphs.

The coefficient of discharge in equation 1 is computed from measurements which include the water-surface levels at an approach section and at the most contracted section, the combined width of the openings, and the discharge. For a given discharge and total width of openings, the variation of the coefficient of discharge is therefore dependent only upon the variation of the surface levels. Compara-

tive measurements of these surface levels, in which the opening-width distribution is varied, are thus indicative of the effect of opening-width distribution upon the discharge coefficient of equation 1.

Surface levels were measured in a series of tests in which a constant total-opening width of 7 feet was contained in either one, two, four, five, or seven symmetrically located openings. During the series of tests, the discharge and tailgate setting remained constant. The tests were made in a smooth 14-foot rectangular flume, using plate constrictive elements. The upstream water-surface level, h_a , was measured at the same distance upstream from the constriction for each test. This distance was equal to the sum of the opening widths—that is, 7 feet. The downstream level, h_3 , is the average of two measurements. The measurements were made at the downstream face of the constriction, and adjacent to the sidewalls of the flume. For tests involving more than one opening, as well as a single opening, this definition of h_3 was assumed to be an adequate measure of the average piezometric head in the live streams at section 3 for all openings. In this connection, it should be noted that the surface levels at the embankments adjacent to the central openings may be depressed below the levels used to define h_3 because of the vortex motion. The results of these tests are shown in plate 4A, in which the variation of h_a , h_3 , and Δh_a is related to the number of openings and the ratio $1 - \frac{\Sigma b}{B}$. The variation of h_a^* and h_3^* , representing the differences between the constricted and the normal levels at sections a and 3, respectively, are also shown. These quantities are of interest in connection with the backwater problem, which is discussed in the latter portion of this report.

The results of a second series of similar tests, in which the channel boundaries were roughened by the addition of chain-link fencing (Manning $n=0.025$) are shown in plate 4 B and C. These tests involve four different total-opening widths, each of which was contained in either one, two, or three separate openings. From the results of these tests, the variation of h_a^* and h_3^* is related to the number of openings and the channel-contraction ratio. The variation of $\frac{h_a^*}{\Delta h_a}$ and $\frac{h_3^*}{\Delta h_a}$ is shown in plate 4C.

For all of the tests shown in plate 4, Δh_a decreases as the number of openings is increased from one to two. As the number of openings is further increased from two to three, Δh_a either decreases slightly or remains constant. From plate 4, it may be concluded that Δh_a , and therefore C , does not change as the number of openings is increased from three to four or more.

Quantitative conclusions regarding the variation of the coefficient of discharge with the change in the number of openings are complicated by certain characteristics of the free surfaces. A change in Δh_a is frequently accompanied by a change in h_3 , and therefore by a change in the gross flow area of the openings, $y_3 \Sigma b$. Thus, in equation 1 the change in C will depend upon the relative influence of the changes in Δh_a and $y_3 \Sigma b$. A change in y_3 will likewise affect the Froude number, one of the other independent ratios of equation 1 [$y_3 / \Sigma b$ has been excluded from consideration].

The relative change in the discharge coefficient as the number of openings is increased from one to two is shown in figure 17. The test

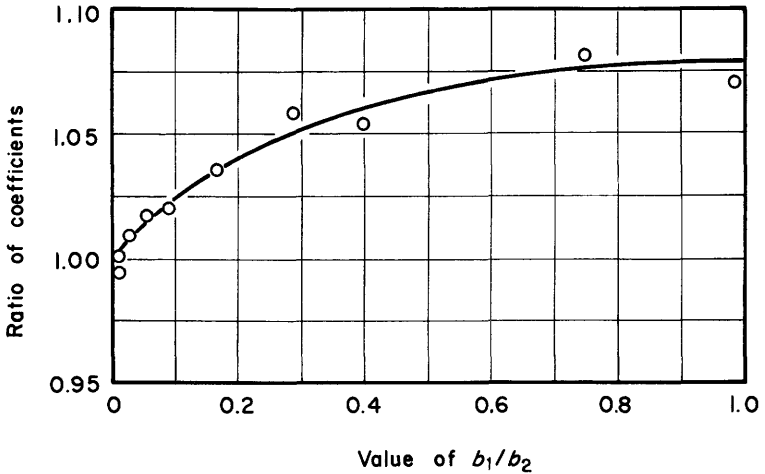


FIGURE 17.—Variation of discharge coefficient with opening-width ratio, two-opening constriction.

results shown in figure 17 were obtained from a third series of tests. For these tests the discharge and the tailgate setting were constant and equal to the values used in the corresponding tests shown in plate 4A. The surface levels were measured as they were in the first series of tests. The 7-foot constant-opening width, which was used in the first series of exploratory tests, was investigated first as one opening, then as two openings of various unequal widths. Initially, one opening of the two-opening constriction was made very small. It was subsequently increased by increments until the two were equal. The limits of the effect shown by this sequence of tests are represented by the one- and two-opening data shown in plate 4A. A one-opening constriction corresponds to a two-opening width ratio (b_1/b_2)=0. The ordinate scale of figure 17 is the ratio obtained by dividing the observed value of the discharge coefficient by its value for the limiting condition of a one-opening condition (that is, for $b_1/b_2=0$). Figure 17 thus shows the relation between the discharge coefficient and the

surface levels at section 1 and section 3. With reference to plate 4 and the slight change in water levels between two-opening constrictions and three-opening constrictions, it is concluded that the increase in C shown in figure 17 represents very nearly the maximum effect due to increase in the number of openings. Thus, the maximum increase in C as compared with single openings is about 7.5 percent.

The effect of the change in Froude number for this particular series of tests is probably very small. The effect of a similar change upon the discharge coefficient for single-opening constrictions (Kindsvater and others, 1953) is approximately 1 percent. A greatly different result is not to be expected in the tests just discussed.

The exploratory tests furnish fairly conclusive evidence that the effect of the distribution of opening width may not be ignored. The tests are of interest, also, in indicating the probable magnitude of this effect.

The possibility of an experimental determination of the limit of subdivision at which the discharge coefficient reaches its terminal value has been considered. Subsequent experiments have shown that the limit is not susceptible to precise or simple determination. For this reason, an alternate approach is outlined in the section of the report to follow.

SEPARATE-OPENING PROCEDURE

A practical solution of the discharge equation for the flow of water through single-opening constrictions has been presented by Kindsvater and others (1953). If it is assumed that the multiple-opening constriction is made up of a series of independent, single-opening constrictions, the discharge characteristics of the individual openings may then be defined in terms of the variables found to be pertinent in the earlier work. This method requires that pseudo-channel boundaries be located in the flow reach upstream from each of the openings to simulate the actual upstream boundaries of the single-opening constriction. Once a logical system for the location of these boundaries has been found, the variation of the discharge coefficient for each opening may then be determined experimentally as in the previous study. Obviously, such boundaries must be so located as to characterize adequately the actual pattern of flow.

DIVISION INTO SINGLE-OPENING UNITS

The upstream flow boundaries may be located by first apportioning the width of each embankment in direct proportion to the gross flow areas of the openings on either side, the larger portion of the embankment being assigned to the larger opening. Lines are projected upstream parallel to the mean direction of flow from the points on

the embankments thus determined. For computation, the lines are assumed to represent the fixed, solid upstream boundaries of an equivalent single-opening constriction. It should be pointed out, however, that these lines frequently are not representative of the true state. At the constriction embankments they are reasonably close to the points at which the flow separates; elsewhere, they rarely coincide with the actual limits of the separate flow regions. They do, however, provide an adequate and unambiguous means of dividing the constriction into independent single-opening units.

COEFFICIENT OF DISCHARGE

The coefficient of discharge for the single-opening unit is

$$C = \frac{q}{A_3 \sqrt{2g \left(\Delta h + \frac{\alpha_1 V_1^2}{2g} - h_{f_{1-3}} \right)}} \quad (2)$$

In equation 2, q is the discharge through an individual opening. Section 1 for each of the openings is located one opening width upstream from the constriction, normal to the mean direction of flow, and is included between the lines which represent the upstream flow boundaries defined in the preceding section. The definitions of the remaining variables in equation 2 are identical with those used previously for single-opening constrictions. Thus, V_1 is the mean velocity in section 1; α_1 is a kinetic-energy correction coefficient; Δh is the difference in water-surface level between sections 1 and 3; $h_{f_{1-3}}$ is the head loss due to friction from section 1 to section 3; and A_3 is the gross flow area of the opening at the downstream side of the constriction and is defined as the product of the opening width and the average depth at section 3.

DETERMINATION OF h_1

The surface level, h_1 , is the average water-surface elevation at the approach section, section 1, for each opening. In the laboratory, water-surface elevations could be measured at any point along section 1. In field application, however, high-water marks are commonly found only along the edge of the channel and the embankment. If this is the case, the values of h_1 for the central openings may be estimated from the observed stagnation levels on the interior embankments. The stagnation levels, h_s , suitably adjusted to account for intervening boundary friction losses and for the velocity head at section 1, may be transferred upstream to the location of the approach section appropriate to each opening.

The intervening friction loss may be estimated by first assuming that the normal velocity component varies linearly with the distance

from the boundary on which the flow stagnates (Prandtl, 1952, p. 62) (Rouse, 1959, p. 45). We write, therefore,

$$V = -cx. \tag{3}$$

In equation 3, V is the mean velocity of the fluid particles which eventually stagnate on an embankment face, x is the normal distance from the face to the particle which moves with velocity V , and c is a constant. The loss over the distance L_w (equal to the opening width, b) is

$$h_f = \int_0^{L_w} S_f dx. \tag{4}$$

The slope of the energy-grade line, S_f , may be evaluated from the Manning equation:

$$S_f = \frac{A^2 V^2}{K^2} \tag{5}$$

where, A , V , and K pertain to the channel and flow properties on the flow-division line in the approach section. Substituting equations 5 and 3 into equation 4, we have

$$h_f = \int_0^{L_w} \frac{A^2 c^2 x^2}{K^2} dx.$$

Assuming that A and K do not vary with x from section 1 to the embankment face, we may substitute A_1 for A and K_1 for K ; thus,

$$h_f = \frac{A_1^2 c^2 L_w^3}{3K_1^2}.$$

At $x = L_w$, $V = -cL_w = V_1$. Then,

$$h_f = \frac{1}{3} \frac{V_1^2 A_1^2}{K_1^2} L_w. \tag{6}$$

Equation 6 is thus an expression for the friction loss along the flow-division line between section 1 and the upstream face of the constriction. In actual computations, the quantities A_1 , V_1 , and K_1 must be approximated by using the average values at section 1 of the two flow channels adjacent to this line; for example, B_1 and B_2 in figure 16. Therefore, h_1 may be determined as

$$h_1 = h_s - \alpha_1 \frac{V_1^2}{2g} + \frac{V_1^2 A_1^2}{3K_1^2} L_w. \tag{7}$$

Equation 7 is found to give reasonable results when applied to the laboratory data. Figure 18 shows a comparison of the computed value

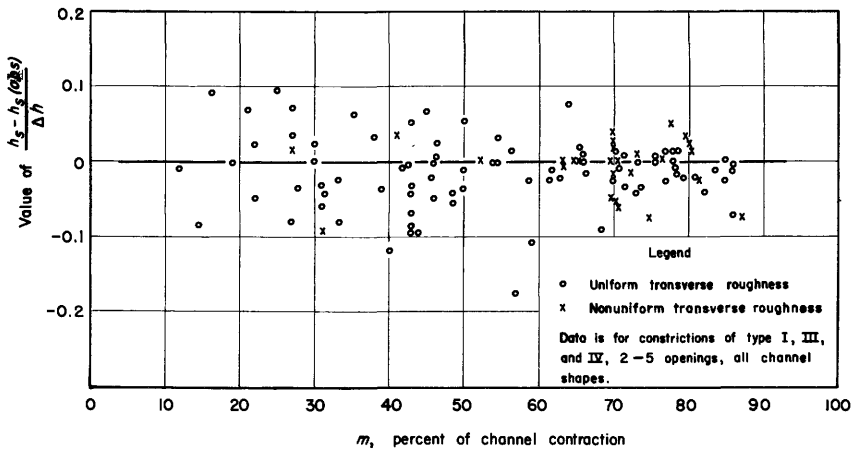


FIGURE 18.—Comparison of computed and observed stagnation levels.

of h_s (from eq. 7) and the actual observed value. The deviations are expressed in percent of Δh for the reason that they also imply the measure of the relative accuracy of this procedure in connection with the determination of discharge.

DETERMINATION OF h_3

The downstream water-surface level, h_3 , is the average of two water-surface levels measured at the downstream faces of the embankments, one on each side of the live stream. Those tests made in smooth channels in which the downstream vortex motion was great enough to cause appreciable surface fluctuations have been excluded.

VARIATION OF DISCHARGE COEFFICIENT

The coefficient of discharge is assumed to be a function of the independent variables defined in the previous study for the single-opening constrictions. Thus:

$$C = f \left(m, \frac{L}{b}, \frac{r}{b}, \phi, \frac{x}{b}, j, F, \theta, e, E, \frac{W}{b}, \frac{y_a + y_b}{2b} \right). \quad (8)$$

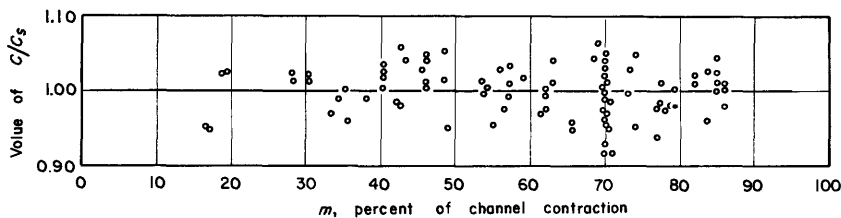
Definitions of the quantities involved in the above equation are given on pages 120–122.

Although it was not anticipated that the discharge coefficients for the individual openings would correspond numerically with those for the single-opening constrictions, this has been found to be the case. Because of this, the presentation of the results is facilitated by comparing the discharge coefficients computed from the laboratory data for multiple-opening constrictions with those for single-opening constrictions. In the charts that follow, the results of the comparison

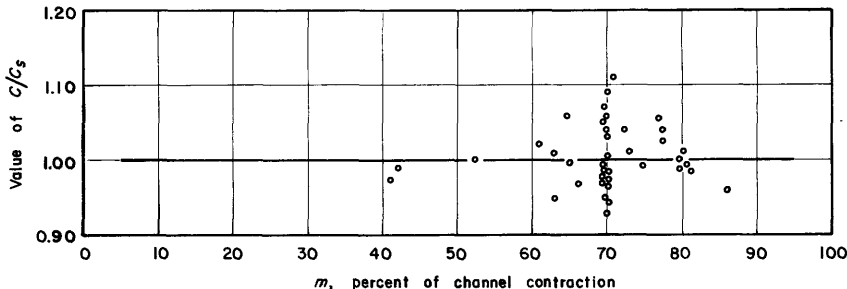
are indicated by the ratios C/C_s , in which C is the observed coefficient for each of the openings computed from equation 2, and C_s is the coefficient of an equivalent single-opening constriction—that is, a single-opening constriction having identical variables: $m, \frac{L}{b}, \frac{r}{b}, \frac{x}{b}, \phi, \theta, e, F$, and so on.

For the purpose of defining the discharge characteristics of the individual openings, it has been presumed that each flow region may be considered independently of the effect of any of the others. It is expected that any fallacies in the premise, as well as inadequacies in the proposed method for separating the flow region, will be indicated by (a) an inconsistent correlation of the ratio of the discharge coefficients with the independent variables shown in equation 8, and by (b) the correlation of the ratio with variables other than those included in equation 8. To verify the assumption, it is thus sufficient to show that the ratio of the discharge coefficients is uniquely defined in terms of the independent variables of equation 8.

The results of tests involving two-opening, vertical-faced constrictions with either rounded or square entrances (type I) are represented in figure 19, in which the ratio C/C_s is shown as a function of the percentage of channel contraction, m , for convenience. “ m ” is defined in the conventional manner as $(1-K_q/K_Q) 100$ (see Kindsvater



A. Uniform transverse roughness, $n=0.025$



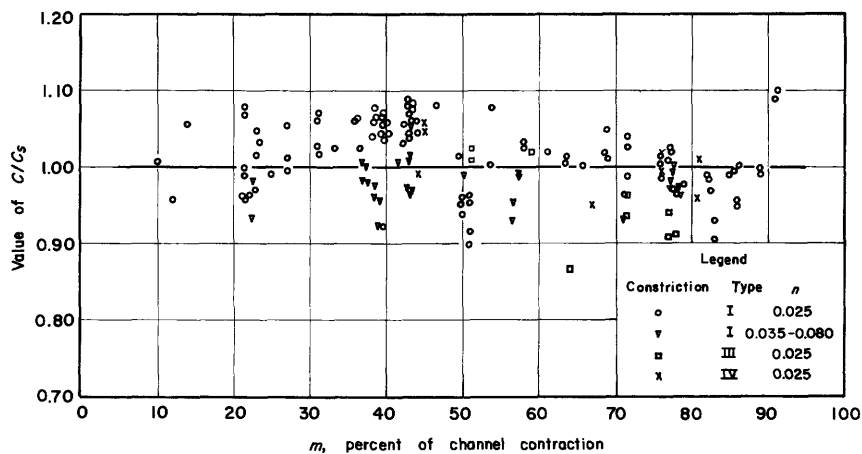
B. Nonuniform transverse roughness, $n=0.012-0.100$

FIGURE 19.—Comparison of coefficients for two-opening constrictions in a rectangular channel.

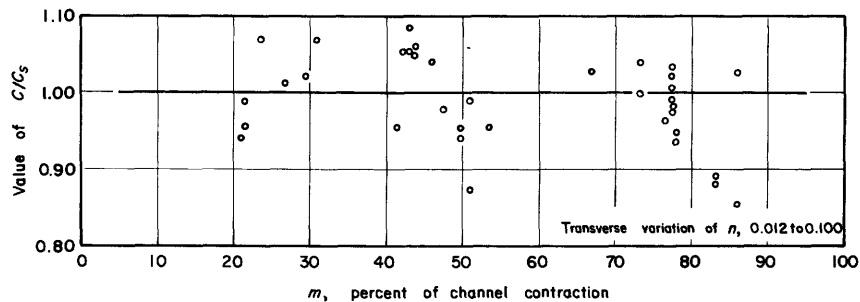
and others, 1953). In this connection, it should be pointed out also that the values of K_v and K_Q for each opening are those included within the fictitious boundaries established by the method described previously. The tests were made in the 14-foot rectangular flume. The floor of the flume was either covered uniformly with roughness material, or covered with various combinations of roughness material ranging from smooth to very rough. Values of n ranged from 0.012 to 0.10. All smooth-boundary tests in which the vortex influence was sufficient to cause large fluctuations in downstream surface level have been excluded.

In these tests, the Froude number at section 3, F_3 , was varied from 0.2 to 0.8; the L/b ratio from 0 to 1.0; and the r/b ratio from 0 to 0.25.

The results of similar tests involving three-, four-, and five-opening constrictions in rectangular channels are shown in figure 20. Finally,



A. Uniform transverse roughness



B. Nonuniform transverse roughness

FIGURE 20.—Comparison of coefficients for 3-, 4-, and 5-opening constrictions in rectangular channels.

the test results obtained in nonrectangular channels are shown in figure 21. The geometry of the nonrectangular channels is shown in figure 22. Figure 21 includes test results for which the transverse

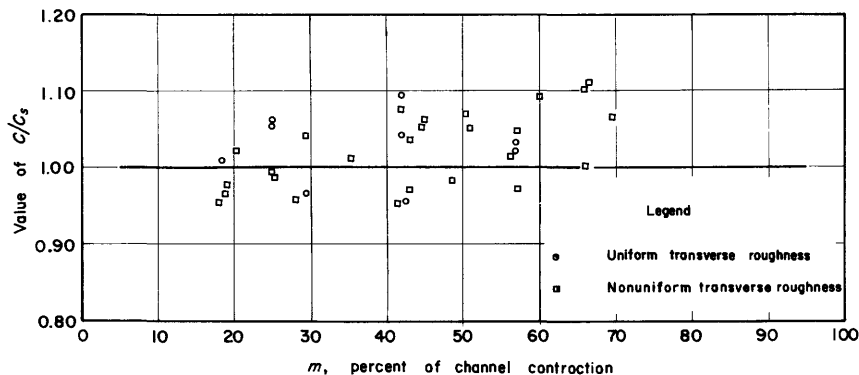


FIGURE 21.—Comparison of coefficients for 2- and 3-opening constrictions in nonrectangular channels.

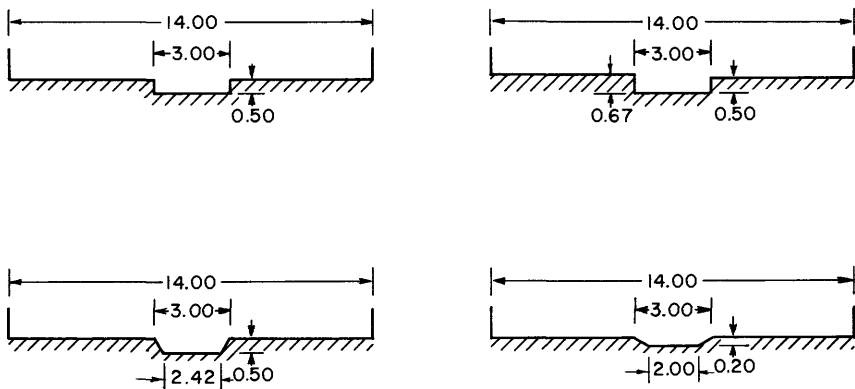


FIGURE 22.—Variation in channel shape.

distribution of roughness was either uniform or nonuniform. Also included are tests on constrictions having sloping embankments, sloping abutment faces, and rounded entrances (type III); and those with sloping embankment faces, vertical abutment faces, and wingwall entrances (type IV). A summary of the range in the geometric and hydraulic variables involved in figures 18-20 is shown in table 1.

In a subsequent analysis (not shown), the ratio C/C_s was also correlated with ratios descriptive of the location of the openings and the embankments. No systematic variation of the ratio with any combination of these variables was disclosed. It is therefore concluded that the method used to locate the upstream flow boundaries is adequate. This result, together with the fact the numerical value of C/C_s varies within acceptable limits, is evidence that the variables

TABLE 1.—Range in geometric and hydraulic variables

GEOMETRIC						
Variable						Range of variation
Channel shape						See fig. 21.
Channel width						feet.. 2-14
Roughness:						
Value of n						0. 012-0. 115
Width of roughness strips						feet.. 1-14
L						do.. 0-9. 04
y_2						do.. 0. 10-1. 21
r						do.. 0-0. 75
W						do.. 0-0. 75
θ						degrees.. 0-60
ϕ						do.. 0-45
Embankment width, in feet:						
Number of openings	s_1	s_2	Range of variation		s_5	s_6
			s_3	s_4		
1	0-10. 70	0-10. 70				
2	0- 9. 75	. 15- 9. 70	0-8. 50			
3	. 35- 5. 60	. 30- 5. 50	. 30-5. 50	0. 35-5. 60		
4	. 75- 4. 39	. 75- 2. 50	. 75-2. 50	. 75-2. 50	0. 75-4. 38	
5	. 70- 3. 61	. 15- 2. 00	. 15-2. 00	. 15-2. 00	. 15-2. 00	0. 70-3. 61
HYDRAULIC						
Variable						Range of variation
Froude number (F_3)						0. 160-0. 806
Discharge						cfs.. 0. 23 -8. 69

included in equation 8 are sufficient to describe the variation of the discharge coefficient.

The ratio C/C_s is a measure of the relative accuracy of the solution. The deviation of the ratio from a value of unity is attributed to experimental error, and to slight differences in the interrelations between the variables used to describe the flow patterns to which the two coefficients pertain. The relative accuracy indicated in figures 19-21 compares favorably with the solution obtained for the single-opening constrictions.

FLOW DISTRIBUTION

In the preliminary design of a multiple-opening bridge, it is frequently necessary to predict the distribution of a given discharge among the openings of a constriction. The variables that control the distribution are obviously the same as those that influence the rate of flow through each opening.

For the flow-distribution problem, the constricted-surface profile is not known. The basic data consist of the total discharge, the normal (unconstricted)-surface level at section 3, a description of the channel and constriction geometry, and information pertinent to the hydraulic roughness of the channel in the vicinity of the constriction. In addition, the charts that describe the variation of the coefficient of discharge for the separate openings are available. From these data, the distribution of the flow is to be predicted.

The discharge through any individual opening of a constriction, related to the total discharge, is

$$\frac{q_i}{Q} = \frac{q_i}{q_1 + q_2 + q_3 + \dots + q_n} \tag{9}$$

The letter q represents the individual-opening discharge. Each q may be expressed in terms of the measured or computed quantities involved in the discharge equation:

$$q = CA_3 \sqrt{2g \left(\Delta h + \frac{\alpha_1 V_1^2}{2g} - h_{f_{1-3}} \right)} \tag{10}$$

In equation 10, CA_3 is the "effective" or live-flow area of an individual opening. The radical quantity represents the average live-stream velocity.

Equation 9 may be rewritten

$$\frac{q_i}{Q} = \frac{(CA_3)_i}{\Sigma(CA_3)} G \tag{11}$$

in which

$$G = \frac{\left[\sqrt{2g \left(\Delta h + \alpha_1 \frac{V_1^2}{2g} - h_{f_{1-3}} \right)} \right]_i \Sigma(CA_3)}{\left[\left[CA_3 \sqrt{2g \left(\Delta h + \alpha_1 \frac{V_1^2}{2g} - h_{f_{1-3}} \right)} \right]_1 \right. \tag{12}$$

$$\left. + \dots + \left[CA_3 \sqrt{2g \left(\Delta h + \alpha_1 \frac{V_1^2}{2g} - h_{f_{1-3}} \right)} \right]_{n-1} \right]}$$

This expression may be interpreted as the ratio of the live-stream velocity at opening i to the average of all live-stream velocities.

An empirical solution of equation 11 has been obtained from the experimental data. For the solution, the ratio q_i/Q was first correlated with the ratio of live-flow areas, $(CA_3)_i/\Sigma(CA_3)$. The result of the correlation is shown in figure 23. The discharge ratio was computed from laboratory measurements of discharge. The opening areas were computed from measurements of h_3 , b , and the average bottom elevation at the openings. The coefficient C was computed from equation 10. The data included the result of tests on the 2-, 3-, 4-, and 5-opening constrictions, made in both rectangular and nonrectangular channels. The channel floor was either smooth, uniformly rough, or nonuniformly rough in the transverse direction.

From equation 12, the value of G is related to the comparative values of the algebraic sums of Δh , $\alpha_1 V_1^2/2g$ and $h_{f_{1-3}}$ for the separate openings. The differences in these sums are associated, primarily, with differences in the resistance characteristics of the component parts of the approach reach related to the separate openings. They are relatively independent of the variables descriptive of the accelerated motion through the openings.

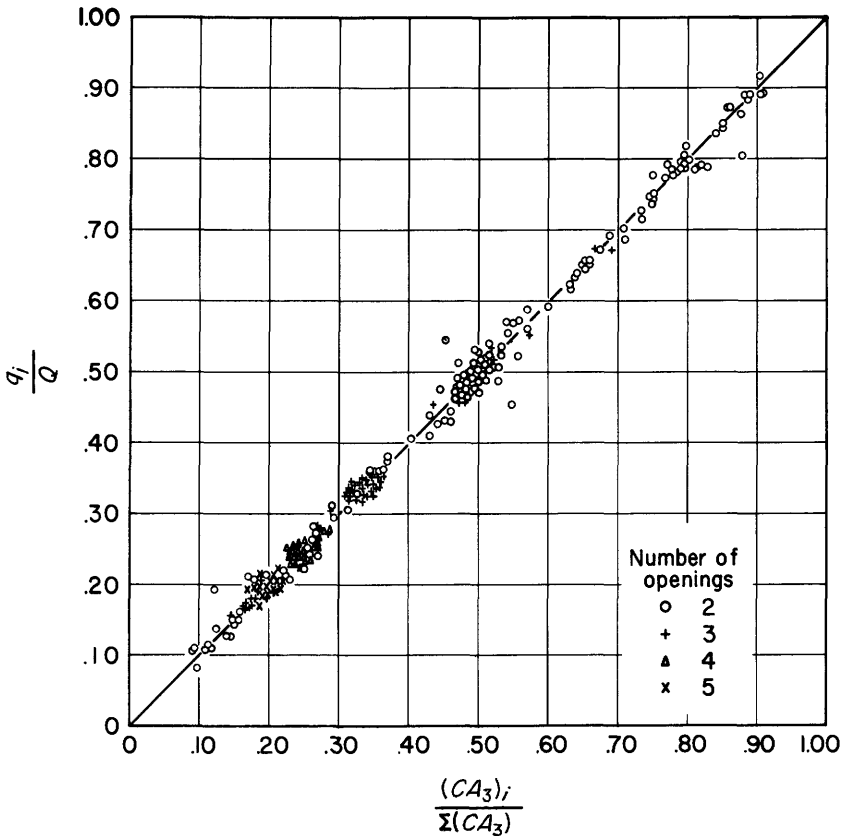


FIGURE 23.—Influence of effective-opening area on discharge distribution.

A measure of the average resistance properties of each approach channel is furnished by the conveyance per unit of area; an approximation of the value of G is thus obtained by relating the unit conveyance of an individual opening to the unit conveyance of the total channel. The conveyance-area ratio is

$$\frac{(K_1/A_1)_i}{\sum K_1/\sum A_1}$$

The areas and conveyances of this ratio are those which apply to the approach sections located in accordance with the procedure outlined in the section of the report concerning the discharge for the separate openings.

The deviations from the line in figure 23, $\frac{q_i/Q}{(CA_3)_i/\sum(CA_3)}$, are next related to the conveyance-area ratio in figure 24.

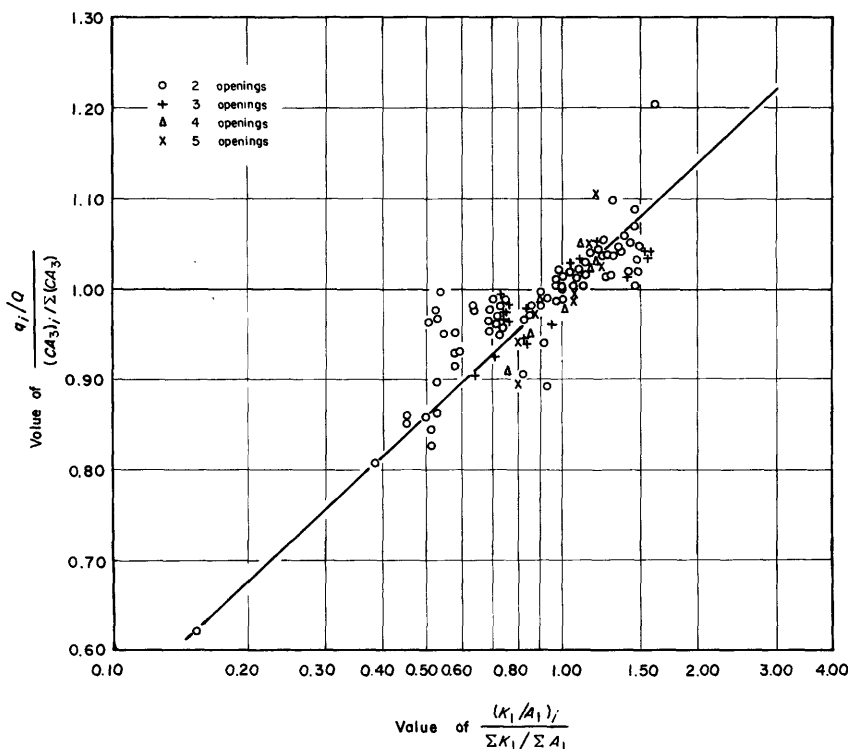


FIGURE 24.—Effect of relative channel roughness on distribution of discharge.

The experimental error involved in the measurement of the opening discharges in the laboratory probably does not justify the further refinement of these results. The trend shown on the figure is believed to be valid, and the average result is perhaps more reliable than the individual points used to define it.

The results of figure 24 represent a solution for equation 11. They are directly applicable to the problem of flow distribution only if the constricted level at section 3 is known. For this purpose, a satisfactory estimate of the difference between the normal and constricted level at section 3 (h_3^*) may be obtained from the equation

$$h_3^* \approx \frac{Q^2}{6g[\Sigma(CA_3)]^2}. \quad (13)$$

In equation 13, Q is the channel discharge. The normal-surface level at section 3 may be used in the estimation of A_3 , and in the selection of C from the report by Kindsvater and others (1953).

The backwater methods, presented in the final section of this report, depend to some extent upon a knowledge of the flow distribution. The values of q_i/Q (from figure 24) based upon the estimate of h_3 from

equation 13 and the relation $h_3 = h_{3n} - h_3^*$ will usually differ by a negligible amount from those obtained from a more precise evaluation of h_3 . They are, however, sufficiently reliable to be used without further correction in the backwater solution. The backwater solution may, in turn, be used to verify the value of h_3^* obtained from equation 13.

BACKWATER EFFECTS

An effect of constricting an open channel is an increase in the water-surface level in the reach upstream from the constriction, and a decrease in level immediately downstream (fig. 16). An evaluation of the difference between the normal and the constricted profiles, the backwater, is of interest to those who are concerned with the prediction or reconstruction of flood profiles.

Because of its use as a reference section in the preceding pages, the nominal approach section—section 1, one opening width upstream from each opening—is perhaps the most convenient location for the measurement of the backwater effect. Unfortunately, however, in almost all cases of multiple-opening constrictions, the section that marks the beginning of acceleration and consequent drawdown of the approaching flow is farther upstream from the constriction than the width of even the largest of the openings of a given constriction. Section 1 is therefore not well suited to an evaluation of the maximum backwater effect. On the other hand, the laboratory tests indicate that the length of the approach reach may be adequately approximated by a distance equal to the combined widths of all the openings, Σb , measured along the centerline of the channel. The location of this section is indicated in figure 16 by the symbol a . The difference in surface levels between the normal and backwater profiles at section a is the backwater measure adopted. This difference in surface level has been designated by the symbol h_a^* in figure 16.

A convenient dimensionless backwater ratio may be formed by dividing h_a^* by Δh_a , the difference in surface elevation between section a and section 3. The variation of the ratio $h_a^*/\Delta h_a$ has been defined experimentally for the separate openings of multiple-opening constrictions.

In the laboratory, the general test procedure for backwater measurements consisted of the observation of the surface level at selected points in the backwater reach. This was done, first with the constriction in place, and then with the constriction removed. The constricted-profile observations were made also as a part of the study of the discharge characteristics of the constriction. The normal-surface profiles were measured following each of the constricted-test runs. The constriction and flume arrangements for the backwater tests are

thus identical with those described in the previous sections of this report.

In the following discussion, curves are developed that show the variation of the backwater ratio for the individual openings. Next, the computation of Δh_a is described. Finally, an alternate backwater solution is outlined, which is restricted to a simplified constriction geometry.

SEPARATE-OPENING PROCEDURE

The magnitude of the backwater ratio, $h_a^*/\Delta h_a$, has been found to depend upon the channel-contraction ratio, m , and upon the entrance geometry of the opening. Also, the variation of the ratio is a function of the arrangement of the openings of the constriction.

BACKWATER-CONTRACTION FACTOR

The distribution of the discharge upstream from section a is a function of the hydraulic characteristics of the stream channel. At the constriction, however, the distribution is controlled by the size, location, and entrance geometry of the openings. In the region between section a and the upstream side of the constriction, therefore, the channel-controlled flow pattern is modified to reflect the boundary influences imposed by the constriction. A measure of the extent of the redistribution process is provided by a comparison, at successive downstream sections, of the hydraulic properties of those parts of the approach channel occupied by the separate-opening discharges.

In the laboratory, dye tracers were used to locate the quasi-boundaries of the separate-opening flow regions in the approach reach and at the constriction embankments. A generalized description of the position of the boundaries is precluded by the infinite number of possible arrangements of channel and constriction. Their location may therefore be approximated at only two sections in the approach reach: at section a and section 1.

At section a , the limits are found by first computing the discharge-distribution ratio for each opening in accordance with the methods already outlined. The total conveyance $\left(K = \frac{1.486}{n} AR^{2/3}\right)$ of the channel at section a is then apportioned in accordance with the relative discharges to locate the limits of each subchannel. For preliminary computations, the unstricted-surface level h_{an} may be used instead of h_a without serious error. The constricted level at section 3 (necessary to the determination of the distribution ratios) may be computed with sufficient accuracy from equation 13.

A method for defining the limits of section 1 was described on page 101.

The backwater-contraction factor, M , for each individual opening of a multiple-opening constriction is used in the computation of backwater at section a and is defined as

$$M = \left[1 - \frac{K_a K_i}{K_i K_a} \right] 100,$$

or

$$M = \left[1 - \frac{K_a}{K_a} \right] 100. \quad (14)$$

BACKWATER RATIO, BASIC CONDITION

Laboratory test data were first selected to define the backwater ratio for simple constrictions in rectangular channels. The constrictions were made up of vertical-faced embankment sections with square entrance corners. The backwater ratio for the basic condition is shown in figure 25A as a function of the factor M . The results shown in this figure are for tests involving constrictions having from two to five openings. The channel floor was uniformly rough. The value of the Manning n for the channels was equal to or greater than 0.025.

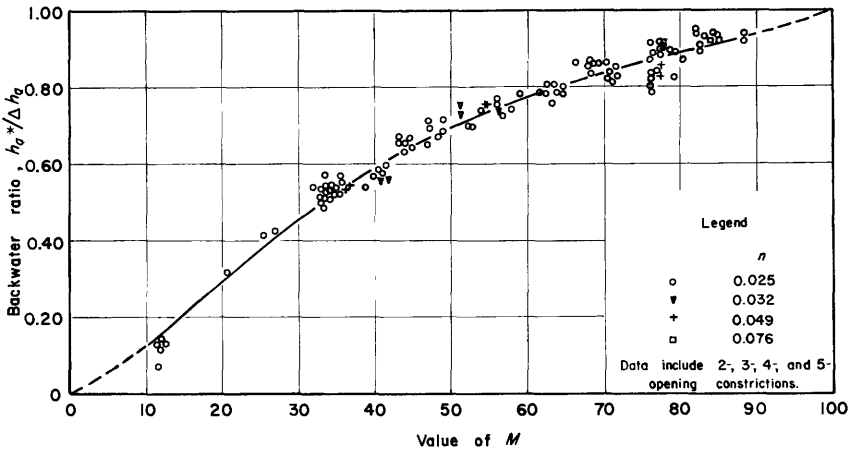
Similarly, figure 25B shows the results of tests made in nonuniformly rough, either nonrectangular or rectangular channels. The constrictions were of the basic type—that is, vertical faced, with square entrances. The curve drawn on figure 25A has been superimposed on figure 25B.

For constrictions of the basic type, the backwater ratio $h_a^*/\Delta h_a$, in figure 25, is a unique function of M . The variation of the ratio appears to be independent of any influence of channel roughness and configuration not incorporated in the factor M . Any effects of Froude number, depth of flow, and the L/b ratio are also largely insignificant.

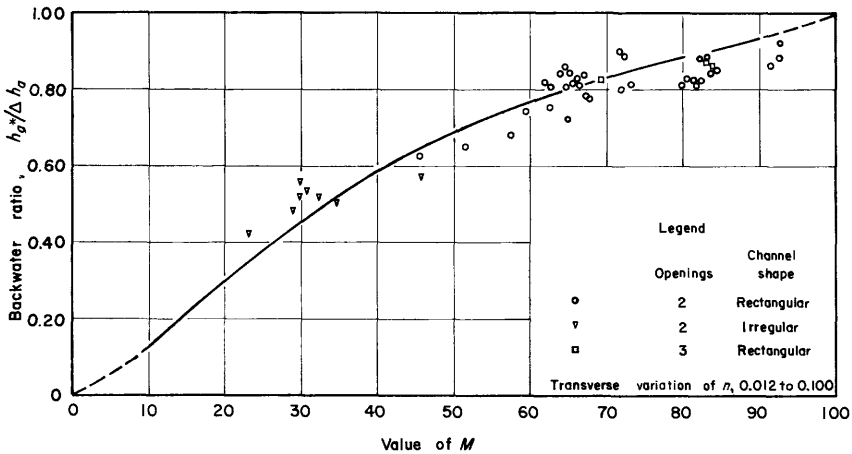
EFFECT OF CONSTRICTION GEOMETRY

The backwater ratio for constrictions of the basic type is defined in figure 25. In addition, a limited number of tests were made with constrictions other than the basic type to determine the influence of constriction geometry on the backwater ratio. These include tests on constrictions with vertical faces having rounded or wingwall entrances. Also included are constrictions having sloping faces (types III and IV).

These tests, without exception, gave numerically smaller values of the backwater ratio than the tests on the basic-type constrictions. This result, which was also found to exist in the single-opening case, is not unexpected. For a given value of Δh , the magnitude of h_1^* (or h_a^*) is a measure of the efficiency of the downstream recovery



A. Uniform transverse roughness, rectangular channel



B. Nonuniform transverse roughness, all channels

FIGURE 25.—Backwater ratio for basic-type constrictions; 2, 3, 4, and 5 openings.

process—the greater the upstream backwater, the greater is the part of Δh lost in the downstream reach. For “ideal-fluid” flow, Δh is equal to h_3^* and h_1^* is zero. For a given opening discharge in real-fluid flow, the combined diffusion and boundary friction losses in the downstream reach are a function of the degree to which the live stream is contracted—the greater the contraction, the greater the losses; and the greater, therefore, the change in the upstream surface elevation. It follows that any change in boundary conditions—such as an im-

provement in entrance geometry—that causes the contraction of the flow entering the opening to be diminished will result in a decrease in the upstream backwater. Moreover, because the quantity Δh_a will decrease also, the resulting smaller numerical value of the ratio $h_a^*/\Delta h_a$ is an indication that h_a^* is affected to a greater relative extent by such a change than is Δh_a .

Thus for constrictions other than the basic type, the change in the backwater ratio may be correlated with a measure of the change in constriction geometry. Because the variation of the discharge coefficient is dependent, primarily, upon constriction geometry, the backwater ratio for the basic constriction may therefore be related to the backwater ratio for the other constrictions by an index factor that is the ratio of the discharge coefficients for the two cases. The adjustment factor for the backwater ratio is called k_c .

The adjustment factor, k_c , has been computed from the results of measurements on the nonbasic-type multiple-opening constrictions, and from the curves given in figure 25. The computed k_c values were then compared with similar adjustment factors (that is, constrictions having identical values of m and ratios of discharge coefficients) developed during a study of single-opening constrictions (Tracy and Carter, 1955, fig. 7). The results are shown in figure 26. It is concluded, from this comparison, that the factors developed for the single-opening constrictions are also applicable to the computation of backwater for the separate openings of the multiple-opening constriction.

The backwater ratios for the nonbasic-type constrictions, so adjusted by the factor k_c selected from Tracy and Carter (1955, fig. 7), are shown in figure 27. The curve drawn on figures 25A and 25B is also superimposed on figure 27.

EVALUATION OF Δh_a

In practice, the difference in surface level between sections a and 3, Δh_a , may be computed from the energy relation

$$\Delta h_a = \frac{q^2}{2gA_3^2C^2} - \alpha \frac{V_a^2}{2g} + h_{f_{a-3}}. \quad (15)$$

In equation 15, q is the individual-opening discharge, A_3 is the gross area of the opening, and C is the discharge coefficient (selected from Kindsvater and others, 1953). The boundary friction loss, $h_{f_{a-3}}$, may be computed from the equation

$$h_{f_{a-3}} = h_{f_{a-1}} + h_{f_{1-3}}. \quad (16)$$

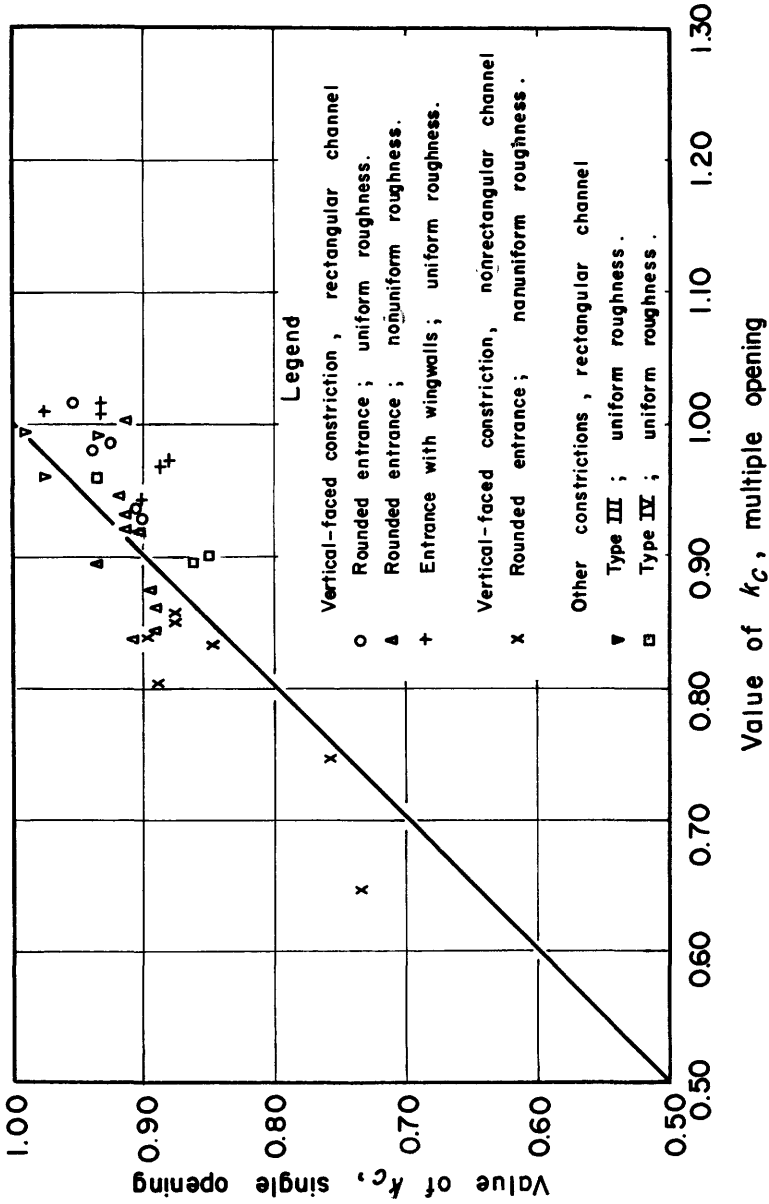


FIGURE 26.—Comparison of k_c for single- and multiple-opening constrictions.

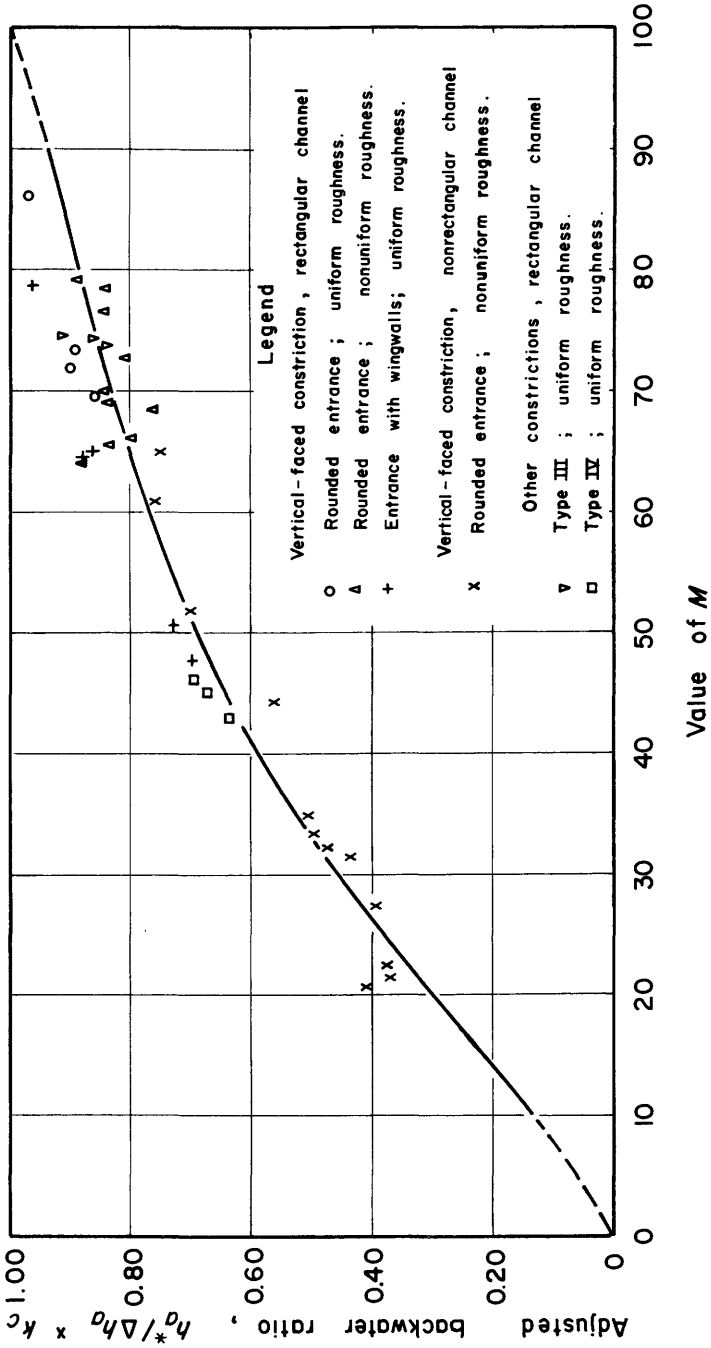


FIGURE 27.—Backwater ratio for separate openings, nonbasic-type constrictions.

Values of $h_{f_{a-1}}$ and $h_{f_{1-3}}$ may be approximated as follows:

$$h_{f_{a-1}} = L_{a-1} \frac{q^2}{K_a K_1}; \quad (17)$$

$$h_{f_{1-3}} = L_w \frac{q^2}{K_1 K_3} + L \left(\frac{q}{K_3} \right)^2. \quad (18)$$

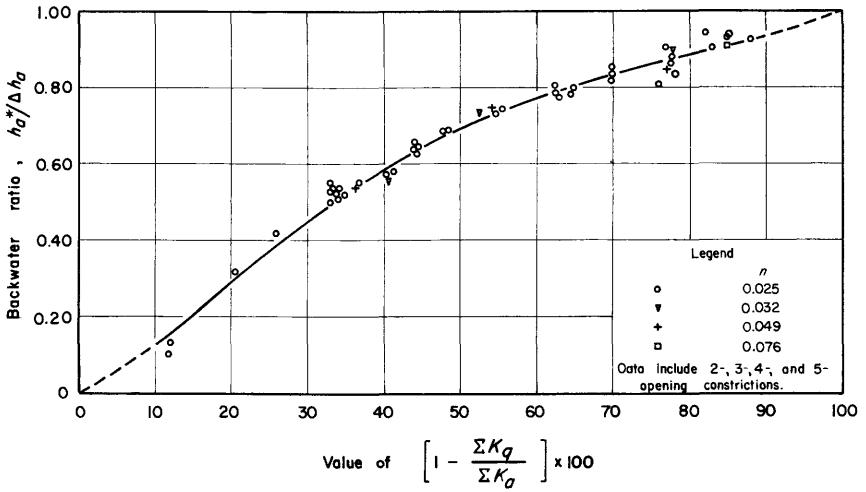
In equations 17 and 18, L_{a-1} is the distance between sections a and 1, and L_w is the distance between section 1 and the constriction. The conveyances, K_1 , K_a , are for those of the parts of the channel occupied by the discharge q at sections 1 and a respectively.

MULTIPLE-OPENING PROCEDURE, BASIC-TYPE CONSTRICTIONS

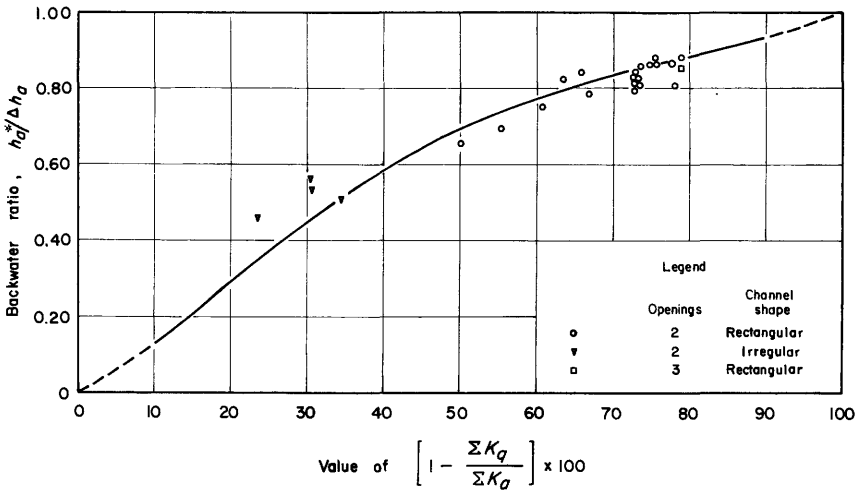
The results of a number of exploratory tests have already been presented (p. 99). The tests were concerned with the effect of opening-width distribution on the variation of the surface levels at selected points in the backwater reach. The tests indicated that both the level at an upstream section and at the downstream side of the constriction were affected to some extent by the opening arrangement. They also indicated, for the channels other than smooth, that the particular backwater ratio shown on plate 4C might be expected to be independent of the effect of this variation.

A reanalysis of the available data for channels other than smooth has been made, in which the backwater ratio $h_a^*/\Delta h_a$ has been related to a contraction ratio based upon the total opening width, Σb . The backwater-contraction factor is $[1 - \Sigma K_q / \Sigma K_a]$. In this connection, ΣK_q is the sum of the conveyance of the projected-opening widths at section 1, ΣK_a is the total channel conveyance at section a , Δh_a is the difference in surface elevation between section a and the average at section 3, and h_a^* is the difference between the normal and constricted level at section a .

Figure 28 shows the results of the reanalysis of the data for basic-type constrictions (vertical-faced, square-edged entrances). In figure 28A, the backwater ratio is shown for channels that are uniformly rough in the transverse direction. Figure 28B shows test results for the cases of nonuniform transverse roughness. The curve drawn on both figures is seen to be the same as that for the backwater from the separate openings (fig. 25).



A. Uniform transverse roughness



B. Nonuniform transverse roughness

FIGURE 28.—Backwater ratio for multiple-opening system, basic-type constrictions.

SYMBOLS

- A Area of section; location of section is denoted by subscript.
- B Width of channel. Also, the width of the part of the channel in the approach reach assignable to an opening.
- b Opening width; the distance between abutment faces. Position of opening is indicated by subscript.

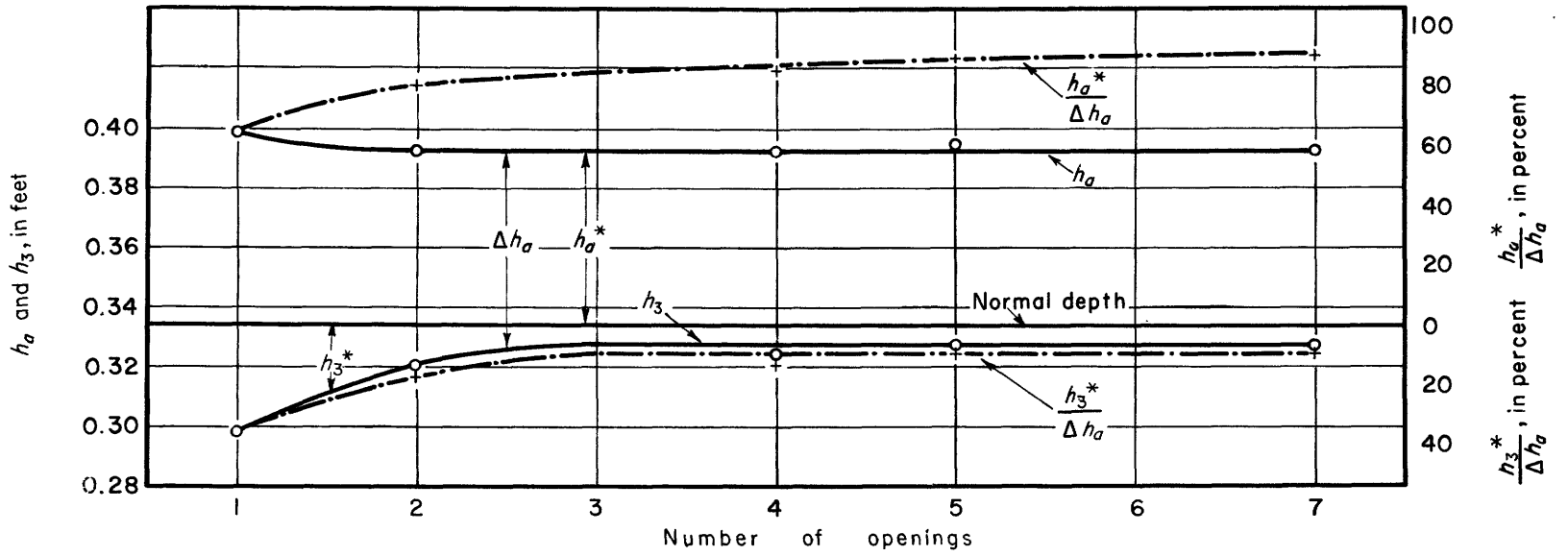
- C* Coefficient of discharge.
- C_s* Coefficient of discharge for single-opening constriction.
- E* Embankment slope.
- e* An eccentricity ratio; see Kindsvater and others (1953).
- F** Froude number; for section 3, $F_3 = \frac{q}{A_3 \sqrt{gy_3}}$.
- G* A discharge ratio divided by an area ratio.
- g* Acceleration due to gravity.
- h* Height of water surface above an arbitrary datum.
- h_s* Stagnation-surface level at embankment face.
- h** Difference between the elevations of the normal- and the constricted-surface profiles. Location of section is denoted by subscript.
- Δh Difference in surface level between an approach section and section 3 for the constricted condition. Location of approach section is indicated by subscript.
- h_f* Boundary friction loss.
- j* The part of the gross area at section 3 occupied by piers or piles.
- K* Channel conveyance; $\frac{1.486}{n} AR^{2/3}$. Location of section is denoted by subscript.
- K_q* Conveyance of the part of section 1 which is located by projecting the opening width directly upstream.
- k_c* An adjustment factor to account for the influence of entrance geometry on the backwater ratio.
- L* Length of abutment.
- M* Backwater-contraction factor.
- m* Channel-contraction ratio.
- n* The Manning coefficient; also, the number of embankment sections.
- Q* Total discharge in stream channel.
- q* Separate-opening discharge. Also, the part of the separate opening discharge which enters the opening without being contracted.
- R* Hydraulic radius.
- r* Radius of rounded entrance corner of the abutment for vertical-faced constrictions.
- S* Width of an embankment section.
- S_f* Slope of the energy-grade line.
- V* Average velocity.
- W* A measure of wingwall length.
- x* Normal distance from constriction face. Also, a variable used in the description of sloping-face embankments.

y	Depth of flow referred to an average bottom elevation.
y_a, y_b	Depth at abutment toes.
α	Kinetic energy correction factor.
θ	Acute angle between a wingwall and the plane of the constriction.
ϕ	Acute angle between the plane of the constriction and a line normal to the average direction of flow.
a	An upstream section that is located at the distance of Σb from the constriction.

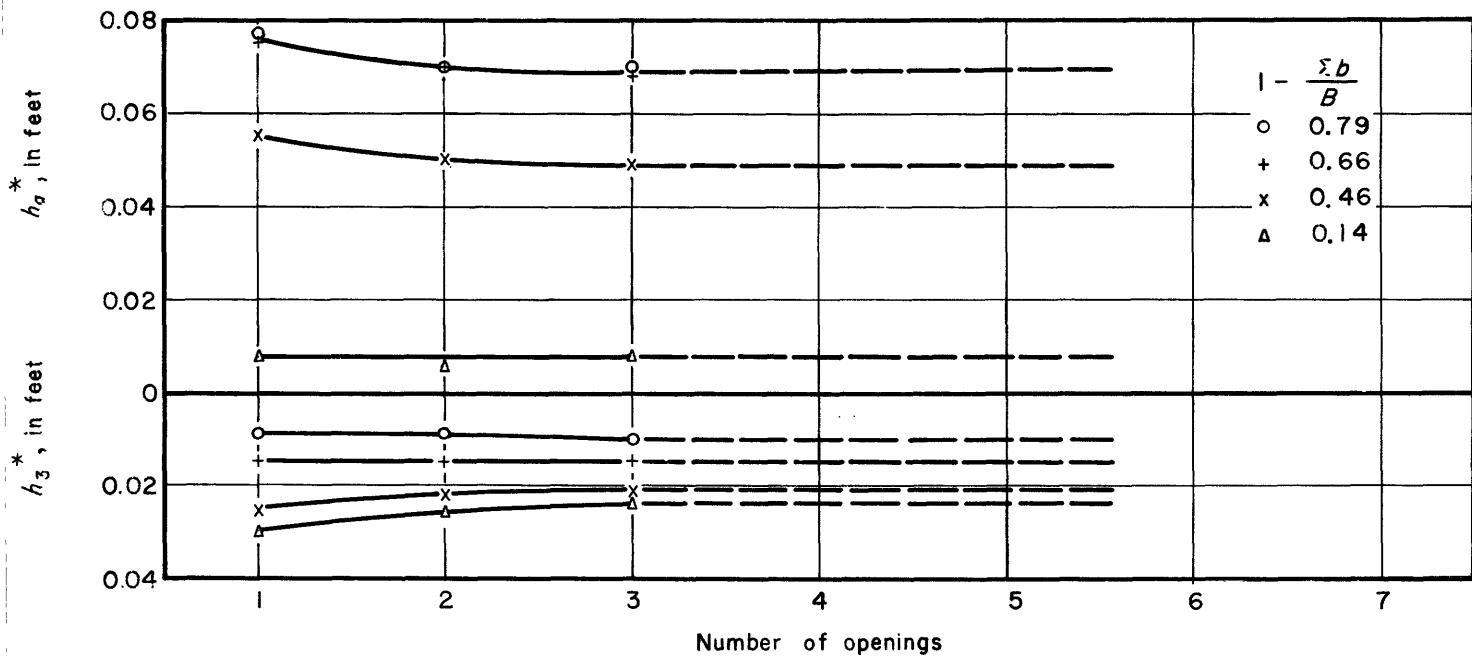
LITERATURE CITED

- Kindsvater, C. E., and Carter, R. W., 1955, Tranquil flow through open-channel constrictions: Am. Soc. Civil Engineers Trans., v. 120, p. 955.
- Kindsvater, C. F., Carter, R. W., and Tracy, H. J., 1953, Computation of peak discharge at constrictions: U.S. Geol. Survey Circ. 284.
- Liu, H. K., Bradley, J. N., and Plate, E. J., 1957, Backwater effects of piers and abutments: Colorado State Univ. Proj. Rept., in cooperation with U.S. Dept. of Commerce, Bur. Public Roads, 364 p.
- Prandtl, Ludwig, 1952, Essentials of fluid dynamics: New York, Hafner Publishing Co., 452 p.
- Rouse, Hunter, 1959, Advanced mechanics of fluids: New York, John Wiley and Sons, 444 p.
- Tracy, H. J., and Carter, R. W., 1955, Backwater effects of open-channel constrictions: Am. Soc. Civil Engineers Trans., v. 120, p. 993.

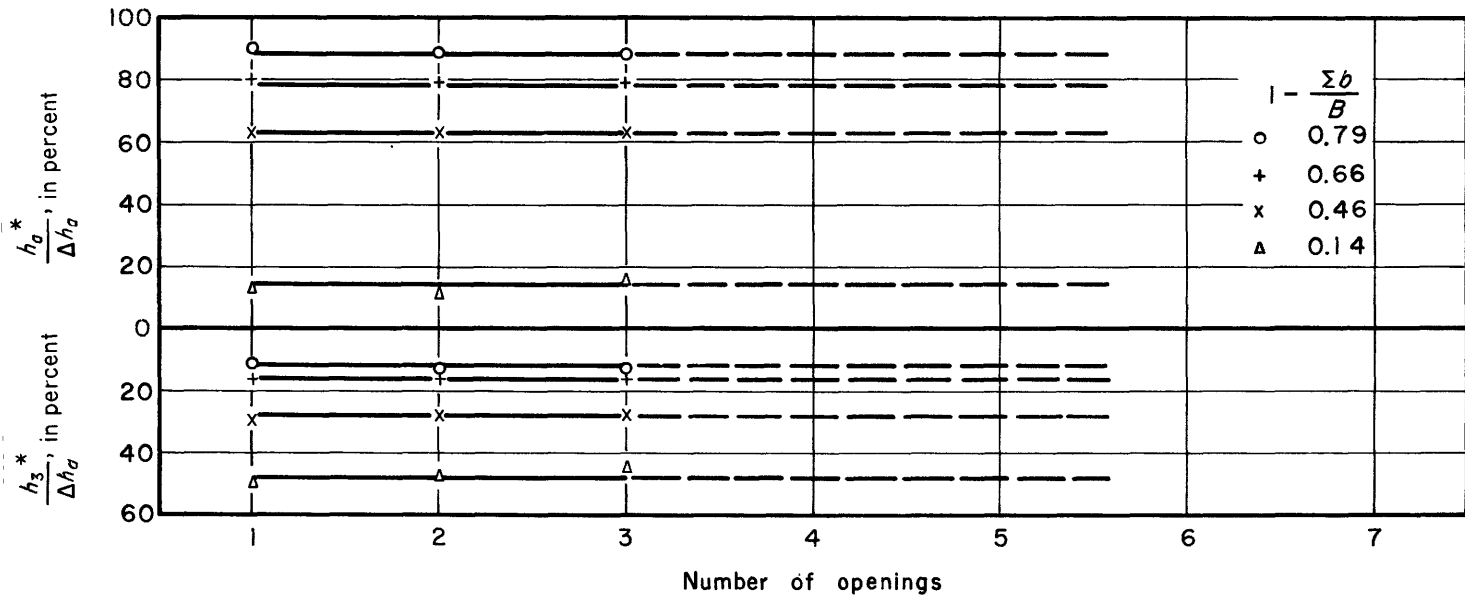




A. Smooth, $1 - \frac{\sum b}{B} = 0.50$



B. Backwater, $n=0.025$



C. Backwater ratio $n=0.025$

VARIATION OF SURFACE LEVEL, BACKWATER, AND BACKWATER RATIO WITH NUMBER OF OPENINGS